P14R.8 THE ROLE OF STORM DYNAMICS ON LIGHTNING ACTIVITY FOR THE 19 JUNE 2004 MESOSCALE CONVECTIVE SYSTEM DURING TELEX

Nicholas S. Biermann, Michael I. Biggerstaff , Gordon D. Carrie, Nicole R. Ramig,
Timothy L. Wiegman, Mark L. Sessing
University of Oklahoma, Norman, Oklahoma

Donald R. MacGorman, W. David Rust
National Severe Storms Laboratory, Norman, Oklahoma

Lawrence D. Carey
Texas A&M University, College Station, Texas

Paul R. Krehbiel, William Rison, Timothy Hamlin
New Mexico Institute of Mining and Technology, Socorro, New Mexico

1. INTRODUCTION

Many studies have been conducted relating lightning flash rates and polarity to the kinematic structure of convective storm systems. Most of these studies have been limited to cloud-to-ground flashes and storm features derived from radar reflectivity (Rutledge and MacGorman, 1988) although a few have also included in-cloud lightning (Boccippio et al. 2001) or total lightning from space-borne optical detectors (Mohr et al. 1996). More recent studies have been able to incorporate polarimetric radar signatures (Carey and Rutledge 2000; Keenan et al. 2000) and data from lightning mapping arrays (Lang et al. 2004) that detect the three-dimensional location of radiation sources along a flash.

While much has been discovered regarding the relationship between kinematic storm structure and lightning activity for individual storms, it has been difficult to generalize the results. Part of the difficulty stems from an incomplete view of the history of the storm's internal structure. In particular, few studies (Keighton et al. 1991) have been able to combine detailed evolution of the storm flow with lightning activity. Earlier work (Billingsley and Biggerstaff 1993) suggested that there is a strong relationship between the changes in the vertical motion within the storm and cloud-to-ground lightning activity.

To develop a more comprehensive understanding of the role of storm dynamics on cloud electrification, an integrated data set was needed that combined the evolution of the storm flow with three-dimensional information on the structure and frequency of lightning flashes, polarimetric radar signatures, and profiles of electric fields within the clouds. This data set was collected during the second Thunderstorm Electrification Experiment (TELEX-2) conducted during May-June 2004 over central Oklahoma (MacGorman et al. 2005).

In this paper we document the internal structure and mesoscale evolution of one of the mesoscale convective systems sampled during TELEX2 and relate the changes to lightning flash rate. We also show preliminary analyses of the lightning flash initiation and termination points relative to the radar reflectivity structure of the cloud system. For the subsection of data shown here, none of the flashes were observed to have originated in the stratiform region although a few cloud-to-ground strikes did occur in the stratiform area.

2. DATA AND METHODS

2.1 Radar Network

The two C-band SMART radars (Biggerstaff et al. 2005) were deployed to the south-southeast of Oklahoma City, OK (Fig 1) on a 46 km baseline. Coordinated data collection began around 1250 UTC and ended around 1600 UTC. The storm propagated from the southwest at a speed of 10 m s^{-1}. The scanning strategy consisted of sector scans to the west as the leading convective line approached and full 360° volume scans once the convective line passed the baseline between the two radars. The sector scans took between 2 to 2.5 minutes depending on the tilt sequence used (Table 1). The full 360°

* *Corresponding author:* Michael I. Biggerstaff, School of Meteorology, University of Oklahoma, Norman, OK 73019; email: drdoppler@ou.edu.

volume scans took 4 minutes to complete. Only sector scans are used here (Table 2).

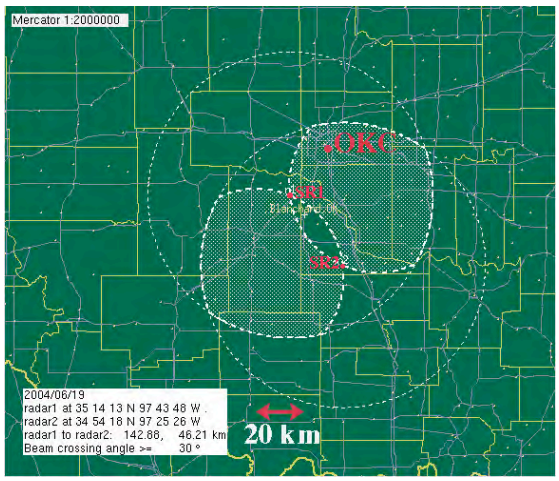

Fig. 1. Location of the C-band SMART radars (SR1 and SR2) during the 19 June 2004 MCS. The location of Oklahoma City, OK is given for reference. The hatched region indicates the area over which the three-dimensional flow can be retrieved from the dual-Doppler analysis. The dashed circles indicate the operational range of the radars.

Table 1. Elevation angles used by the SMART radars during the 19 June 2004 MCS..

130° Sector Near	130° Sector Here
0.5	0.8
0.8	2.1
1.7	4.3
2.8	7.1
4.5	11.3
6.2	15.3
7.9	19.3
9.6	23.0
11.5	27.1
13.4	30.9
15.6	35.0
17.7	38.6
20.0	42.3
22.2	45.7
24.6	48.9
27.4	52.4
30.5	55.8
33.5	58.9

The 100 km operational range of the SMART radars during the 19 June 2004 MCS provided a Nyquist velocity of ± 20 m s^{-1}. Doppler data were edited and dealiased using SOLOii (Oye et al. 1995).

The edited data were interpolated to Cartesian coordinates using REORDER (Oye et al. 1995) with a Cressman weighting interpolation method that employed a beamwidth-dependent radius of influence. The radius of influence varied with range such that high resolution in the region closest to the radar was retained while farther from the radar low resolution occurred. This is consistent with the inherent resolution associated with finite beamwidth radar. The dimensions of the analysis grid extend 110 km in the x (east-west) direction and y (north-south) direction, and from 0.3 to 14.3 km in the z (vertical). The horizontal spacing between points is 1 km and the vertical spacing is 0.5 km.

REORDER output from the two radars were combined and wind fields were retrieved using CEDRIC (Custom Editing and Display of Reduced Information in Cartesian Space; Mohr et al. 1986). Our analysis takes into account a radar reflectivity-based estimated fall speed of the participation particles assuming the particles are either rain, snow, or graupel depending on their altitude and the radar reflectivity. A two-step Leise (1981) filter was applied to the horizontal wind components before computing divergence. This led to a resolvable horizontal wavelength scale of around 6 km. The resolvable vertical scale, determined by the elevation tilts of the volume scans, was ~2-4 km wavelength depending on the range from the radar.

Table 2. Beginning times and types of sectors scans used in the study.

Beginning Time (UTC)
12:52:45 (Near)
12:55:30 (Near)
12:58:16 (Near)
13:01:01 (Near)
13:03:45 (Near)
13:06:31 (Near)
13:09:15 (Near)
13:12:01 (Near)
13:14:45 (Near)
13:26:10 (Here)

The divergence field was integrated downward using a fraction of the integrand as a boundary condition to retrieve vertical motion. A lower boundary condition was also applied and the residual mass flux was redistributed in the vertical column and reintegrated to arrive at an estimate of the vertical velocity. The horizontal winds were corrected for the vertical motion, and the flow

field recomputed iteratively until the solution of the winds converged. Only 3-4 iterations were necessary for the solution to converge.

2.2 Lightning Data

MacGorman et al. (2005) provide details regarding the three dimensional lightning mapping array deployed in central Oklahoma. Here, we make use of a manual analysis of the cloud flashes to extract the location of the initiation and termination points of the flash. For discharges that produced branched flashes, the termination point of each main branch has been determined. Considering the volume of data examined, only two minutes out of every 10-minute period was able to be analyzed manually.

3. STORM STRUCTURE

3.1 Environmental Characteristics

The 19 June 2004 MCS developed in southwestern OK in a region of low-level warm air advection and weak differential vorticity advection associated with a small amplitude short-wave trough at 500 mb. A sounding taken from Norman, OK to the east of the storm initiation region (Fig. 2) shows that the environment in central Oklahoma had not yet fully recovered from convective activity that had occurred earlier. The convective available potential energy (CAPE) was ~ 200 J kg^{-1}. Moreover, there was very little low-level wind shear to aid the organizing the storm system. Hence, the storm system was not particularly vigorous. Farther to the south, the CAPE was higher, reaching 1700 J kg^{-1} in the sounding taken at Ft. Worth, TX (not shown). But the low-level shear was still weak.

Despite the moderately conducive environment, the 19 June 2004 MCS organized into a leading line of convection and produced a trailing stratiform rain region. It retained this structure as it was being sampled by the TELEX2 observing network.

3.2 Radar Reflectivity and Airflow

For the period sampled by the SMART radars, the 19 June 2004 MCS exhibited many of the classic features (Biggerstaff and Houze 1991) of a leading-line trailing stratiform squall line system (Fig. 3). There was a multicellular convective region with older convection towards the rear of the line, a narrow transition zone, and a developing stratiform rain region. A vertical cross-section through the storm (Fig. 4) shows that the upward motion in the strongest convection was ~ 13 m s^{-1}, consistent with the low CAPE environment.

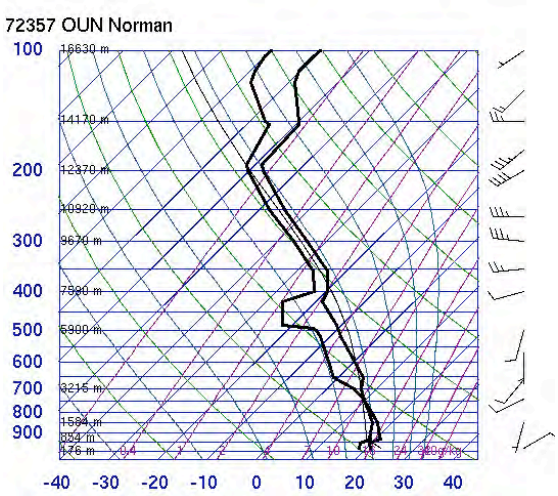

Fig. 2. SkewT-logP sounding taken from Norman, OK at 1200 UTC 19 June 2004. The CAPE was 217 J kg^{-1}.

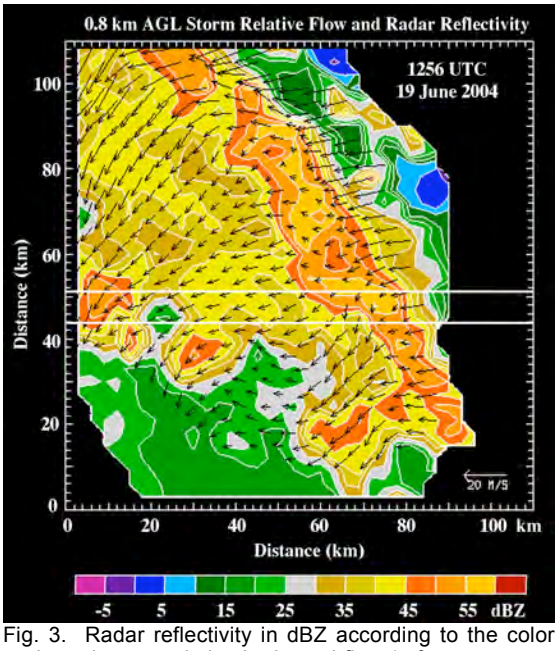

Fig. 3. Radar reflectivity in dBZ according to the color scale and storm relative horizontal flow (reference vector in lower right corner of plot) at 0.8 km AGL and 1256 UTC on 11 June 2004. Horizontal lines indicate location of cross-sections shown in Figs. 4 and 5.

Along-line variability did exist in the strength of the convection and in the depth and magnitude of the storm-relative mid-level rear inflow. In the region from Y=45 to Y= 30 km in Fig. 3 the rear inflow was stronger (not shown), but the convective cells appeared to have been weaker (Fig. 5). It is possible that

the enhanced horizontal vorticity associated with the rear-inflow overwhelmed the horizontal vorticity associated with the environmental inflow (Weisman et al. 1993) leading to a more tilted and weaker updraft in that part of the storm system.

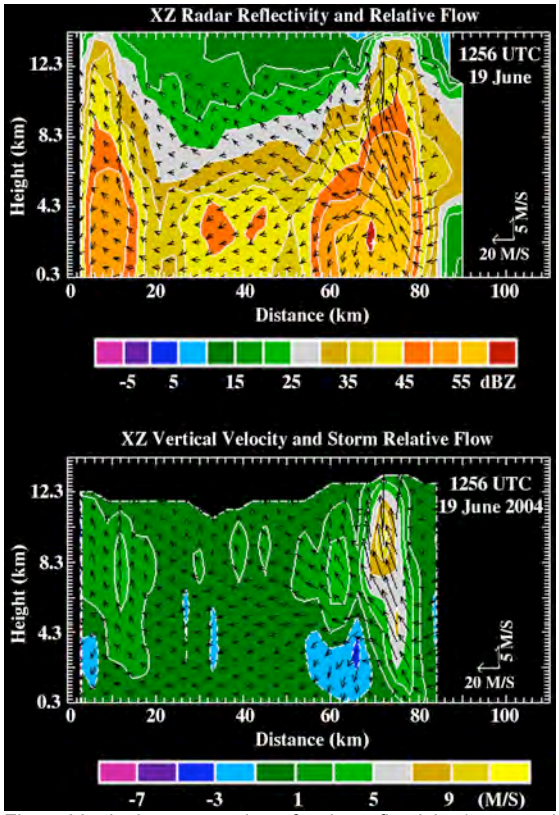

Fig. 4. Vertical cross-section of radar reflectivity (top panel in dBZ according to the color scale) and vertical velocity (bottom panel in m s^{-1} according to the color scale) along the northern line indicated in Fig. 3. Vectors of storm-relative flow in the plane of the cross-section (U and W) have been overlaid.

With time, the rear inflow region expanded northward and the along-line flow at upper levels (not shown) became less line parallel and was directed more towards the rear of the storm system. This aided in the further development of the stratiform rain region. A series of electric field soundings were taken in the stratiform region during its active developing stage (MacGorman et al. 2005).

One non-classic feature of the 19 June 2004 MCS was the embedded convective cells at the rear of the stratiform region. Those cells were deep and contained moderately strong updrafts, compared to convection in the leading line. Later, we will show that these cells did produce lightning flashes.

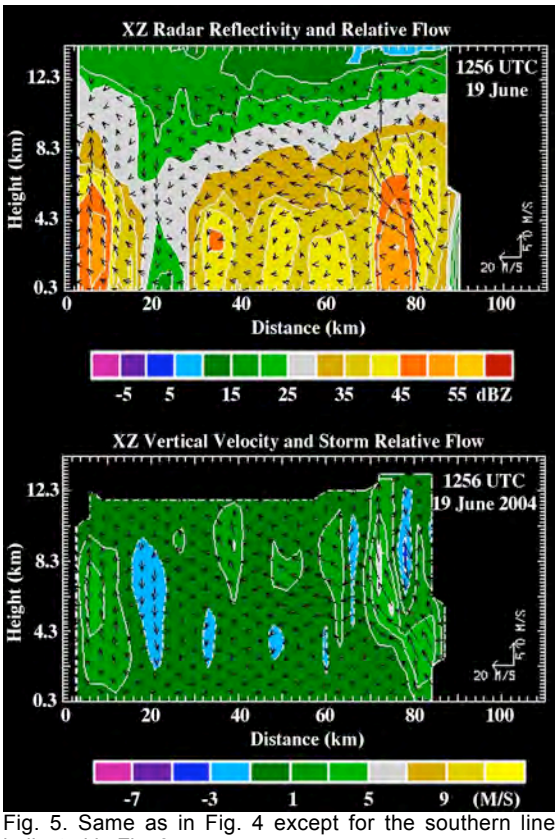

Fig. 5. Same as in Fig. 4 except for the southern line indicated in Fig. 3.

3. LIGHTNING & STORM EVOLUTION

3.1 Mesoscale Variability

Given the relatively low CAPE in the environment east of the genesis region of the storm, it is not surprising that the convective activity weakened during the observational period. Profiles of radar reflectivity, taken over the convective line sampled by the SMART radars, reveal that the mid-to-upper-level area-averaged radar reflectivity decreased by ~ 8 dB in just 30 minutes (Fig. 6). The storm system appeared to re-intensify slightly during the later stages but did not regain its peak strength. At lower altitudes, the radar reflectivity actually increased beyond its initial profile despite the weaker values aloft.

Concurrent with the changes in mid-to-upper level radar reflectivity structure, the overall flash rate of the storm system (Fig. 7) decreased dramatically in the first 30 minutes before increasing slightly to a much less active secondary peak. The later stages again showed a gradual decrease in flash rate consistent with the gradual decrease in mean mid-level radar reflectivity.

Vertical velocities over the convective region during the first 20 minutes of the observational period also decreased (Fig. 8). In fact, much of the decrease occurred in just the first few minutes indicating a relatively rapid decrease in convective draft strength over the mesoscale region sampled by the radars.

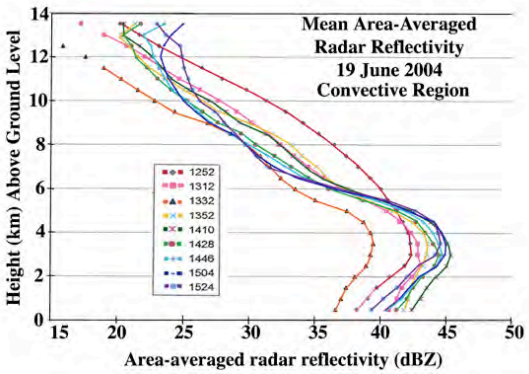

Fig. 6. Vertical profiles of area-averaged radar reflectivity over the convective region sampled by the SMART radars from 1252 to 1524 UTC.

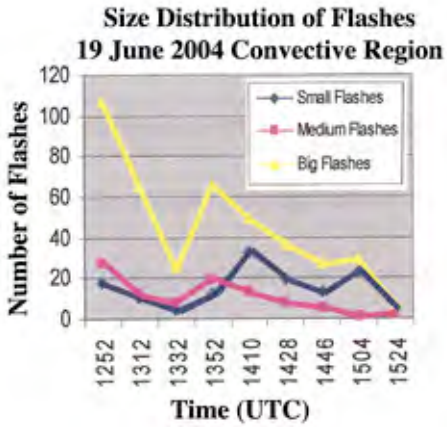

Fig. 7. Total flash rate (number per 3 minute interval centered in time on the mean time of the radar volume scan) for both in-cloud and cloud-to-ground flashes over the convective region sampled by the SMART radars for the 19 June 2004 MCS.

3.2 Convective Variability

Examination of individual lightning flashes revealed that they originated from the convective region (Fig. 9). For the subset of data examined here (127 flashes with 22% being cloud-to-ground), none of the flashes originated within the stratiform cloud. Nevertheless, a few positive polarity cloud-to-ground strikes did occur in the stratiform rain region (Fig. 10). All but one of the stratiform region CGs originated from 6-8 km in the rear portion of the convective line and propagated back into the stratiform area. The other flash originated at 11 km and was associated with the convective cell at the rear of the stratiform region.

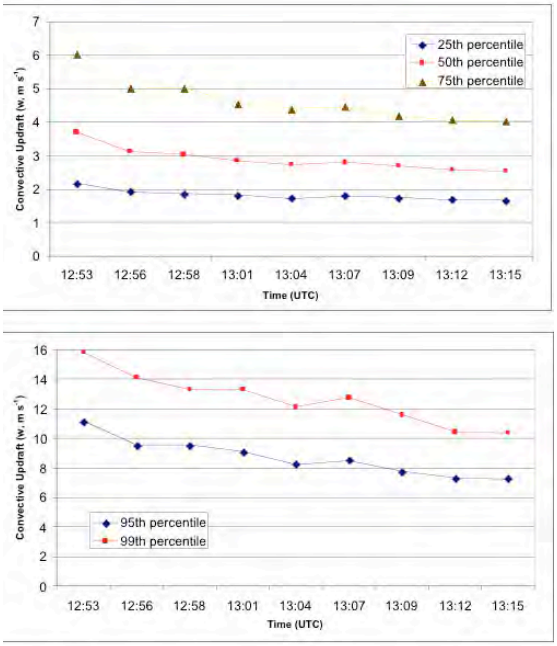

Fig. 8. Statistical distribution of updraft strength as a function of time during the first 20 minutes of the analysis period.

The lightning initiation points seem to occur in regions of high reflectivity gradients along the edges of convective cells. Initiation locations were distributed between the leading edge, middle, and rearward part of the convective line, indicating that lightning can occur in all stages of the thunderstorm lifecycle. Preliminary analysis suggests that discharges along the rear of the convective line tended to propagate into the stratiform region while discharges near the leading edge tended to propagate either along the line or into the forward anvil. If this finding withstands additional scrutiny, it may indicate that the lightning discharge path is related to advection of charged particles by the storm relative flow.

Both positive and negative polarity cloud-to-ground strikes occurred within the convective line with negative strikes accounting for two-thirds of the total cloud-to-ground flashes. All the positive polarity strikes originated from 6-8 km in altitude. The majority of negative cloud-to-ground strikes originated between 3-5 km altitude. A few negative CGs did originate higher, between 8-9 km. But these were a small fraction of the total number of strikes. The vertical

separation of flash initiation zones suggests that the primary electric field structure might be adequately described as a bipole, where a negative charge center lay beneath a positive charge center. This is consistent with the first electric field sounding taken in the convective line for this case (MacGorman et al. 2005).

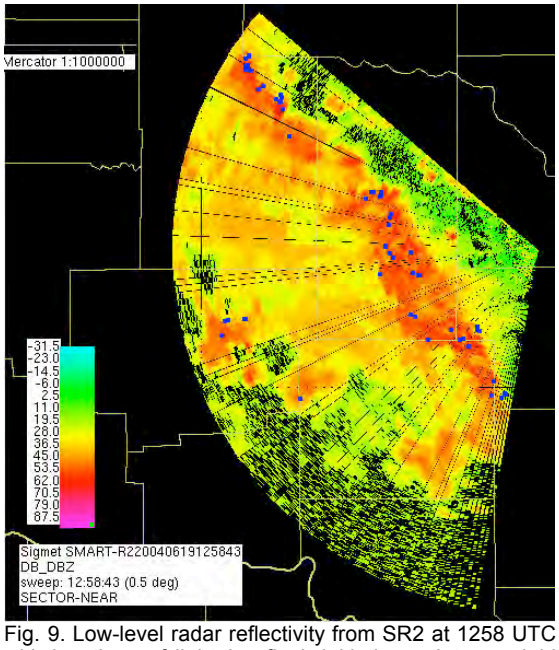

Fig. 9. Low-level radar reflectivity from SR2 at 1258 UTC with locations of lightning flash initiation points overlaid (blue circles). The flashes are from 1258-1300 UTC.

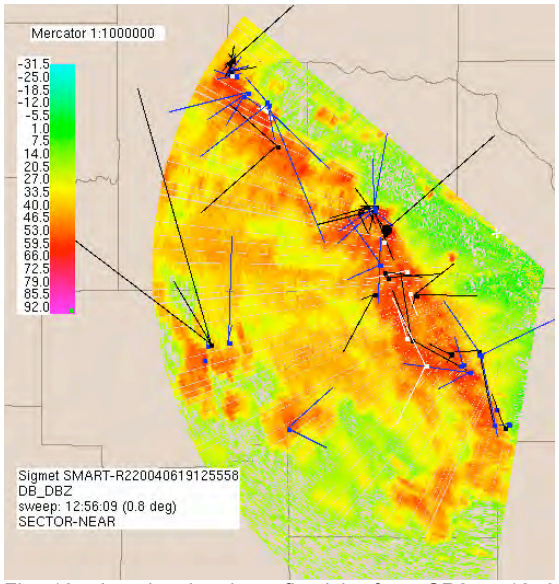

Fig. 10. Low-level radar reflectivity from SR2 at 1256 UTC with lightning initiation points and lines to lightning termination points overlaid. Blue lines indicate all branches of the flash were in-cloud. Black lines indicate that one of the branches was a CG strike. White indicates an inconclusive flash. None of the flashes extending ahead of the line were CGs.

4. CONCLUSIONS

TELEX2 provided an integrated data set that can be used to examine the relationship between storm dynamics and cloud electrification. Here we showed an example of the changes in storm structure and lightning activity for a leading-line trailing-stratiform squall line system that occurred on 19 June 2004 over central Oklahoma. A rapid transition in the strength of the storm with mean radar reflectivity at mid-levels decreasing by ~ 8 dB over a 30-minute period was associated with a rapid decrease in the overall flash rate and a significant reduction in the strength of the convective updrafts over the mesoscale region sampled by the radars.

For the subset of data examined, individual flashes initiated only in convective zones along the edges of convective cells in regions of strong reflectivity gradients. The cloud-to-ground strikes in the stratiform rain region lowered positive charge to ground and originated from 6-8 km in the rear portion of the convective line. The convective line itself contained both positive and negative cloud-to-ground strikes with the majority of the negative strikes originating between 3-5 km in altitude, indicating that the primary charge distribution in the convective line might be bipolar.

5. ACKNOWLEDGMENTS

Support for the SMART radar deployment during TELEX was provided through the Cooperative Institute for Mesoscale Meteorological Studies at the University of Oklahoma and the National Science Foundation under grants ATM-9912562 and ATM-0233268. E. Bruning assisted with the lightning data analysis. C. Alexander provided software for automatic editing of the radar data.

6. REFERENCES

Biggerstaff, M. I. and R. A. Houze, Jr., 1991: Kinematic and precipitation structure of the 10-11 June 1985 squall line. *Mon. Wea. Rev.,* **119**, 3034-3065,

Biggerstaff, M. I., L. J. Wicker, J. Guynes, C. Ziegler, J. M. Straka, E.N. Rasmussen, A. Dogget IV, L. D. Carey, J. L. Schroeder, and C. Weiss, 2005: The Shared Mobile Atmospheric Research and Teaching (SMART) Radar: A collaboration to enhance research and teaching. *Bull. Amer. Meteor. Soc.*, **86**, 1263-1274.

Billingsley, D. B., and M. I. Biggerstaff, 1993:

Evolution of cloud-to-ground lightning characteristics in the convective region of a Mesoscale Convective System. Preprints, *Fifth Symp. on Global Change Studies*, Amer. Meteor. Soc., 340-344.

Boccippio, D. J., K. L. Cummins, H. J. Christian, and S. J. Goodman, 2001: Combined satellite- and surface-based estimation of the intracloud-cloud-to-ground lightning ratio over the continental United States. *Mon. Wea. Rev.*, **129**, 108-122.

Carey, L. D. and S. A. Rutledge, 2000: The relationship between precipitation and lightning in tropical island convection: A C-band polarimetric radar study. *Mon. Wea. Rev.*, **128**, 2687-2710.

Keenan, T., S. Rutledge, R. Carbone, J. Wilson, T. Takahashi, P. May, N. Tapper, M. Platt, J. Hacker, S. Sekelsky, M. Montcrieff, K. Saito, G. Holland, A. Crook, and K. Gage, 2000: The Maritime Continent Thunderstorm Experiment (MCTEX): Overview and some results. *Bull. Amer. Meteor. Soc.*, **81**, 2433-2455.

Keighton, S. J., H. B. Bluestein, and D. R. MacGorman, 1991: The evolution of a severe Mesoscale Convective System: Cloud-to-ground lightning location and storm structure. *Mon. Wea. Rev.*, **119**, 1533-1556.

Lang, T. J., L. J. Miller, M. Weisman, S. A. Rutledge, L. J. Barker III, V. N. Bringi, V. Chandrasekar, A. Detwiler, N. Doesken, J. Heldson, C. Knight, P. Krehbiel, W. A. Lyons, D. MacGorman, E. Rasmussen, W. Rison, W. D. Rust, and R. J. Thomas, 2004: The Severe Thunderstorm Electrification and Precipitation Study. *Bull. Amer. Meteor. Soc.*, **85**, 1107-1125.

Leise, J.A., 1981: A multi-dimensional scale-telescoped filter and data extension package. NOAA Technical Memo, WPL-82, 20pp.

MacGorman, D., D. Rust, C. Ziegler, T. Schuur, E. Mansell, M. Biggerstaff, J. Straka, E. Bruning, K. Kuhlman, N. Ramig, C. Payne, and N. Biermann, P. Krehbiel, W. Rison, T. Hamlin, L. Carey, 2005: Lightning relative to storm structure, evolution, and microphysics in TELEX, Preprints 32nd Confer on Radar Meteor., CD-ROM, Amer. Meteor. Soc., Albuquerque, NM.

Mohr, C., L. Miller, R. Vaughan, and H. Frank, 1986: The merger of mesoscale datasets into a common Cartesian format for efficient and systematic analyses. *J. Atmos. and Oceanic Technol.,* **3,** 143-161.

Mohr, K. I., E. R. Toracinta, E. J. Zipser, and R. E. Orville 1996: A comparison of WSR-88D reflectivities, SSM/I brightness temperatures, and lightning for Mesoscale Convective Systems in Texas. Part II: SSM/I brightness temperatures and lightning. *J. Appl. Meteor.*, **35**, 919-931.

Oye, R., C. Miller, and S. Smith, 1995: Software for Radar Visualization, Editing, and Interpolation. *Preprints, 27th Conference on Radar Meteorology.* Vail, CO. Amer. Meteor. Soc., 359-361.

Rutledge, S. A. and D. R. MacGorman, 1988: Cloud-to-ground lightning: Climatological characteristics and relationships to model fields, radar observations, and severe local storms. *Mon. Wea. Rev.*, **117**, 518–535.

Weisman, M. L., 1993: The genesis of severe, long-lived bow echoes. *J. Atmo. Sci.*, **50**, 645-670.